# Deformation Behavior and Microstructure Effect in 2124Al/SiCp Composite

Ling Zhong

*Journal of Composite Materials* 2000 34: 101
DOI: 10.1177/002199830003400202

# Deformation Behavior and Microstructure Effect in 2124Al/$SiC_p$ Composite

LING ZHONG
*LNM*
*Institute of Mechanics*
*Chinese Academy of Sciences*
*Beijing 100080, P.R. China*

(Received April 14, 1998)
(Revised December 20, 1998)

**ABSTRACT:** Dynamic compression tests were performed by means of a Split Hopkinson Pressure Bar (SHPB). Test materials were 2124Al alloys reinforced with 17% volume fraction of 3, 13 and 37 μm SiC particles, respectively. Under strain rate $\dot{\varepsilon} = 2100$ 1/s, SiC particles have a strong effect on $\sigma_{0.2}$ of the composites and the $\sigma_{0.2}$ increases with different SiC particle size in the following order: 2124Al-alloy → 124Al/$SiC_p$ (37 μm) → 2124Al/$SiC_p$ (13 μm) → 2124Al/$SiC_p$ (3 μm), and the strain hardening of the composites depends mainly on the strain hardening of matrix, 2124Al alloy. The results of dimensional analysis present that the flow stress of these composites not only depends on the property of reinforcement and matrix but also relates to the microstructure scale, matrix grain size, reinforcement size, the distance between reinforcements and dislocations in matrix. The normalized flow stress here is a function of inverse power of the edge-edge particle spacing, dislocation density and matrix grain size. Close-up observation shows that, in the composite containing SiC particles (3 μm), localized deformation formed readily comparing with other materials under the same loading condition. Microscopic observations indicate that different plastic flow patterns occur within the matrix due to the presence of hard particles with different sizes.

**KEY WORDS:** microstructure effect, flow stress, localization, plastic flow pattern, 2124Al/$SiC_p$ composite.

## 1. INTRODUCTION

IN RECENT DECADES, a great deal of attention has been paid to metal matrix composites containing hard particles ($MMC_p$) [1]. It is partly because of that the composites offer potential for significant improvements in mechanical performance over monolithic alloys in many structural applications. While the $MMC_p$ exhibits markedly higher stiffness and strength than the matrix alloys, they often



0021-9983/00/02 0101–15 $10.00/0

suffer from lower ductility and inferior fracture toughness due to the presence of hard and brittle particles. The mechanisms of strengthening, microscopic damage and failure in the $MMC_p$ therefore are issues of academic and practical importance. Many different mechanisms have been proposed which, either independently or concurrently, are considered responsible for the overall strength of the composites [1,2]. Among them, the relation between the strengthening and geometrical variables associated with the particle distribution and matrix microstructure is important.

A considerable body of experimental, theoretical and simulation information is now available on strengthening and microstructure geometrical effects of two phase composites. Previous experimental research was on alloys with second phase particles. In 1962, Edelson et al. [3] presented detailed experimental results and discussed the effect of second phase particles on the mechanical properties of alloys, which involved the influence of particle size, spatial distance and particle volume fraction to the yield stress, fracture stress, ductility as well as hardening of alloys. In the early 1980s, after examining much research on fracture of alloys and based on the theory of continuum media mechanics, Cheng [4] applied the dimensional analysis to the study of microstructure effect, such as second phase particles' size and spatial distribution in the fracture of alloys and indicated that the microstructure scale is important to the fracture of properties of alloy containing second phase particles. Hong et al. [5] investigated experimentally in influence of the particle size and spatial distribution to the fracture of alloys and results agreed with what was analyzed in Reference [4]. In theoretical research, the typical analytical techniques, such as Eshelby's equivalent inclusion method [6,7], have been developed and could describe the composite with two phases or more but they always require idealizations of phase geometry and material behavior which often deviates markedly from real material geometry and response. Similar to alloys, in $MMC_p$, the microstructure effect is still important to mechanical properties. Some of the microstructure effects in $MMC_p$, such as sharp corners of hard particles and higher volume fraction of particles, would make analysis more complex [1]. Therefore, features, such as particles' size, spatial distributions and so on, which have influence on the mechanical properties of the composite, particularly on the local strain fields between reinforcements, should be quantitatively described. Needleman et al. [8–10] applied the continuum model, based on materials with voids, to the study metals containing hard particles. Also, they adopted finite element analysis to simulate overall mechanical response of $MMC_p$, in which the particle shape, size, spatial distribution and non-uniform local stress and strain fields could be accounted for [11,12]. Simply speaking, the above analysis is based on the macroscopic continuum description which is effective as long as the characteristic microstructure dimensions of the composite constituent are small compared to the mean separation distance of the reinforcements and the reinforcement size. Microscopic details that have influence on deformation, such as grain size and

mean dislocation spacing, are not taken into account in these publications. Hirth et al. [13–15] proposed a model involved in microstructure parameters influencing local plastic deformation and presented the effective stress which depends on the inverse power of particle spacing between two neighboring particles in MMC$_p$. The model is consistent with several experimental results.

In order to obtain more essential understanding of the deformation of MMC$_p$ under monotonic loading and of the influence of microstructure in the MMC$_p$, we used Split Hopkinson Pressure Bar (SHPB) to test a group of 2124Al/SiC$_p$ containing SiC particles of three different sizes, 3, 13, and 37 μm. The research focused on the microscopic scale, such as grain size of matrix, reinforcement particle size and spatial distribution, etc., and macromechanical response as well as microscopic images of local deformation fields appearing in presented materials under monotonic impact compression loading. As a comparison, 2124Al alloy without reinforcement particles was investigated also.

## 2. EXPERIMENTAL PROCEDURE

### 2.1 Material and Specimen Preparation

The materials used in this study are 2124Al alloy and 2124Al reinforced with 17% volume fraction of 3, 13 and 37 μm SiC particles. These materials are hot rolled plates about 12 mm thick supplied by BP Metal Composites Ltd. (U.K.). The chemical composition and the standard mechanical properties of the 2124Al alloy, under static tensile loading, are listed in Table 1 and Table 2. Figure 1 is the micrographs of a rolled MMC$_p$, 2124Al/SiC$_p$ (37 μm). SiC particles are aligned along the rolling direction, the smaller the SiC particles, the clearer their alignment. No broken SiC particles, voids or debonding between particles and matrix could be seen, and the matrix grain size is about 3–4 μm.

Before testing, specimens were solution heat tested, i.e., heated to 530°C and held for about 55 minutes then quenched in cold water. To prepare the samples for close-up observation, the specimen was sectioned along the compression axis. The sectioned surface was then fine polished and etched for microscopic examination.

### 2.2 Mechanical Testing

The dynamic compression testing was performed on a Split Hopkinson Pressure Bar (SHPB). A lot of descriptions of SHPB apparatus have been presented so there

***Table 1. Chemical formula of base 2124Al alloy, wt% (after Materials Safety Data Sheet, BP Metal Composites Ltd.).***

| Cu | Mn | Mg | Fe | Zn | Si | Cr | Ti + Zr | Al |
|---|---|---|---|---|---|---|---|---|
| 4.0–4.4 | 1.3–1.6 | 0.4–0.7 | 0.3 | 0.25 | 0.2 | 0.1 | 0.2 | Bal. |

*Table 2. Typical mechanical properties of 2124Al alloy (T4) (static tensile test).*

| Tensile Strength (MPa) | Young's Modulus (GPa) |
|---|---|
| 460 | 72 |

is no need to illustrate it again here [16]. To keep one-dimensional stress in the specimen during loading, compressive specimen is cylindrical with 5 mm diameter and 5 mm high and the rolling direction parallel to the compression axis. Strain rate of 2100 1/s, is chosen for all the tests so that mechanical responses, under the same strain rate, in these composite would be obtained. Data including stress-strain relation curve of each specimen could be obtained by wave profiles recorded.

## 3. EXPERIMENTAL

### 3.1 Mechanical Response

Stress-strain curves of the materials, subjected to dynamic compression (strain rate about 2100 1/s), are summarized in Figure 2. One of the prominent features in these curves is that, under the same loading condition, the flow stress of the materials depends on the SiC particles. The smaller the SiC particles, the higher the flow stress of composites. Among them, the composite, containing 3 μm SiC particles, has the highest flow stress and the matrix material, 2124Al alloy, is of the lowest flow stress under the same loading condition. Usually, the whole deformation process of these materials could be regarded as two parts, elastic and plastic. Some

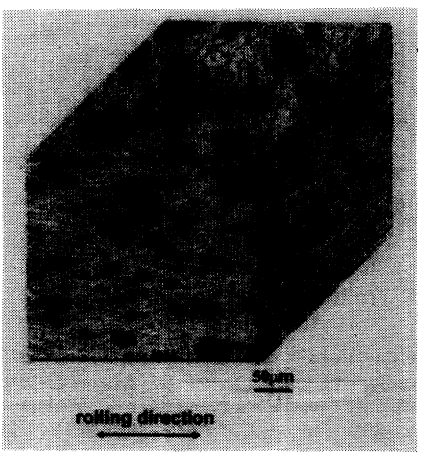


*Figure 1. The micrograph of original material, 2124Al$SiC_p$ (37 μm).*

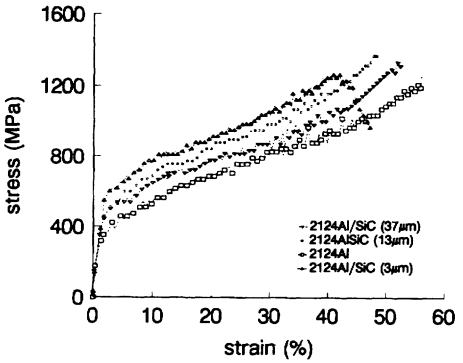


***Figure 2.*** *σ-ε curves of 2124Al and its composites under dynamic compression, $\dot{\varepsilon}$ = 2100 1/s.*

typical stress levels of the materials, such as $\sigma_{0.2}$, $\sigma_{max}$ and so on are listed in Table 3. Comparing the increase of stress in the two stages, the flow stress during the flow stage has increased a lot and almost 2.5 times its $\sigma_{0.2}$ (see the third item in Table 3). For example, at the end of the elastic stage, $\sigma_{0.2}$ of the composite containing SiC particles (3 μm) is about 545 MPa while in the flow stage, at the strain 40%, the flow stress is up to 1250 MPa. At the same strain, however, variations of stresses between 2124Al alloy and its composites do not show obvious changes. In the composite with SiC particles (3 μm), its $(\sigma/\sigma_m)_{0.2}$ is about 1.56 and $\sigma/\sigma_m$ at strain 40% is about 1.42 (see the last two items in Table 3); the difference between the two is about 0.14. For other composites, the difference is smaller, 0.01 for composite with SiC particles (13 μm) and 0.04 for composite with SiC particles (37 μm). It is shown that SiC particles increase $\sigma_{0.2}$ of composites during elastic stage and the increasing levels depend on the sizes of SiC particles. But in the whole deformation process, the stress increasing in the present materials is mostly due to strain hardening in the flow stage, and the strain hardening curves are nearly parallel for all sizes of the SiC particles; that is, the strain hardening of the present composites depends only on that of matrix materials. So the composite containing small SiC particles would keep the highest flow stress during the plastic deforma-

***Table 3. Typical stress levels in the present materials ($\dot{\varepsilon}$ = 2100 1/s).****

| | $\sigma_{0.2}$ (MPa) | $\sigma_{max}$ ($\varepsilon$ = 40%) (MPa) | $\sigma_{0.2}/\sigma_{max}$ | $(\sigma/\sigma_m)_{0.2}$ | $\sigma/\sigma_m$ ($\varepsilon$ = 40%) |
|---|---|---|---|---|---|
| 2124Al alloy | 350 | 878 | 0.40 | 1 | 1 |
| 2124Al/SiC$_p$ (3 μm) | 545 | 1250 | 0.44 | 1.56 | 1.42 |
| 2124Al/SiC$_p$ (13 μm) | 457 | 1160 | 0.39 | 1.31 | 1.32 |
| 2124Al/SiC$_p$ (37 μm) | 444 | 1056 | 0.42 | 1.27 | 1.23 |

*$\sigma_{max}$ is the stress level at strain 40% of each material; $\sigma_m$ is the stress level of 2124Al under the same strain.

tion process. While small SiC particles increase the stress, the ultimate axis strain in the composite is not greater than that of other materials with larger SiC particles or without SiC particles, which could be seen clearly in Figure 2. In 2124Al alloy containing 3 μm SiC particles, the maximum strain is about 40%, over which the stress-strain curve drops down and the specimen seems to be failure, but at the same strain other specimens do not show any evidence of failure according to their curves of stress and strain. Additionally, for the present materials, their elastic modulus did not change obviously with change in the reinforcement size.

### 3.2 Microscopic Observation

Close-up observation for these samples was carried out under VICKERS-55 and NEOPHOT-21 microscopes as well as S-570 SEM. V-shaped and slight dark regions could be seen on the elongation profiles of these samples etched, which were always along the diagonal lines to the profile. Microscopic observation showed that they are deformed regions. In these regions, matrix grains deform while deformation levels and orientations always depend on SiC particle Size. In 2124Al alloy, grains in the deformed region have been distorted and become small strip-like but their orientations are almost along the direction of flow deformation [Figure 3(a)], or along the diagonal line to the profile of the deformed sample. In the composite containing 3 μm SiC particles, a part of aligned particles has oriented along the large plastic flow and formed a narrow band [Figure 3(b)]. The band, about 10 μm in width, is along the tip of the macro-crack. The nearer the tip, the narrower the band. Under the same magnification, the microscopic deformations in the other two composites containing SiC particles of 13 and 37 μm, do not show obvious localization and appear to show only the plastic flow at the matrix between two neighboring particles [Figures 3(c) and (d)]. For example, in the composite with 13 μm SiC particles, matrix grains flow along the diagonal line to the profile of the sample and SiC particles seem to be oriented slightly [Figure 3(c)]. Particularly, in the composite containing large SiC particles (37 μm), obvious plastic flow could be seen at the matrix between two neighboring particles and its flow orientation changed due to large SiC particles' presence; the matrix grains near the corners of the particles have distorted very much compared with those farther away from the particles [Figure 3(d)].

Figure 4 gives a micrograph of microdamage occurring in 2124Al alloy reinforced with 3 μm SiC particles. There is a lot of microdamage, small voids and debonding at the localized deformation region. Most of the voids have been oriented along the direction of shear flow, and most of the debonding is found at the interface between the particle and matrix or the corners of the hard particles. Compared with the other two samples of composites containing 13 and 37 μm SiC particles under the same loading with strain rate of 2100 1/s, a few particle cracks could be seen in the sample containing 3 μm SiC particles. It is noticed that, for the three composites, whether containing small or large SiC particles, microdamage

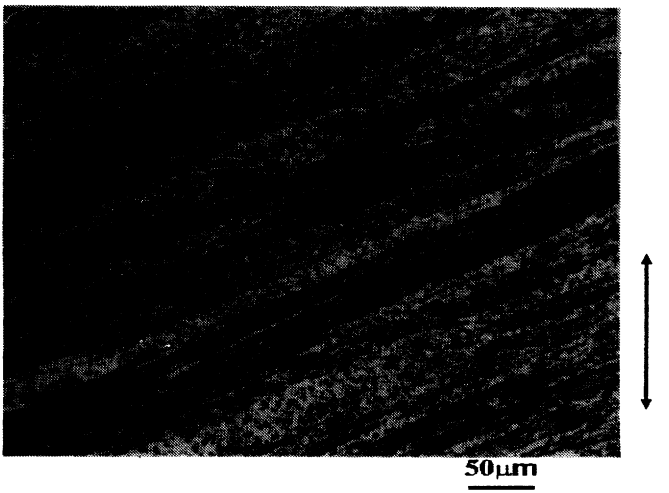


*(a)*

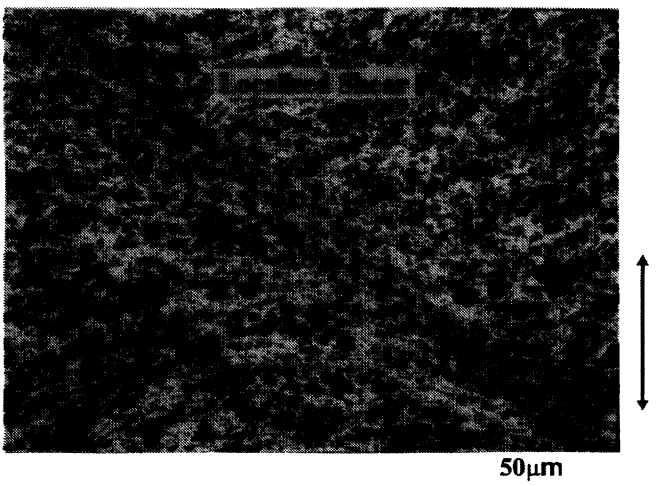


*(b)*

***Figure 3.*** *Micrograph of deformation in 2124Al and its composites under dynamic compression, $\dot{\varepsilon}$ = 2100 1/s, in which the arrow direction is loading direction: (a) 2124Al; (b) 2124Al/SiC$_p$ (3 μm); (c) 2124Al/SiC$_p$ (13 μm); (d) 2124Al/SiC$_p$ (37 μm).*

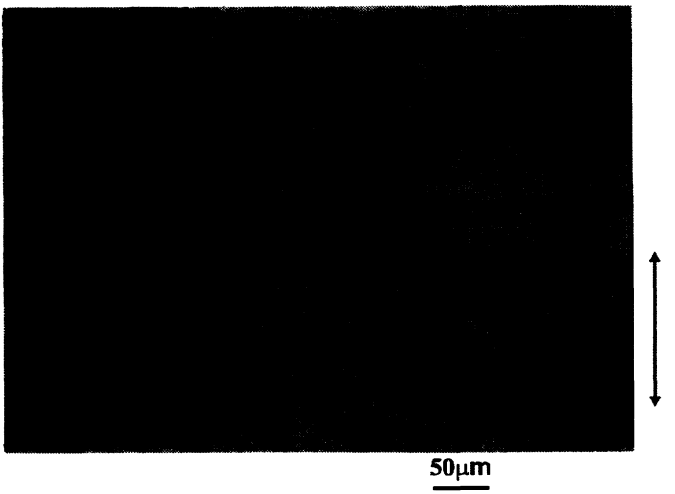


(c)

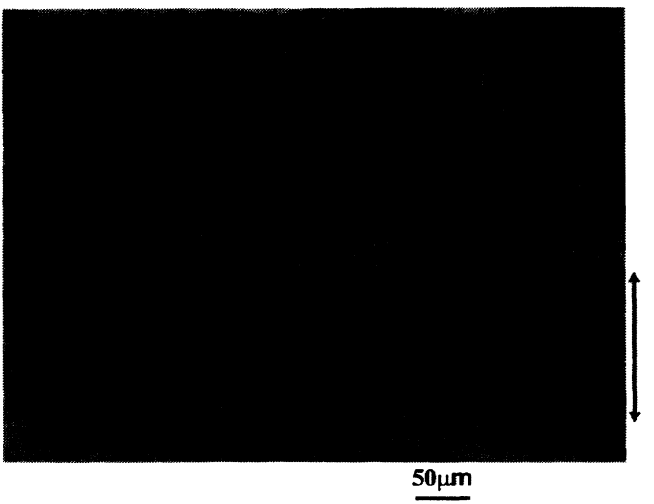


(d)

***Figure 3 (continued).*** *Micrograph of deformation in 2124Al and its composites under dynamic compression, $\dot{\varepsilon}$ = 2100 1/s, in which the arrow direction is loading direction: (a) 2124Al; (b) 2124Al/$SiC_p$ (3 μm); (c) 2124Al/$SiC_p$ (13 μm); (d) 2124Al/$SiC_p$ (37 μm).*

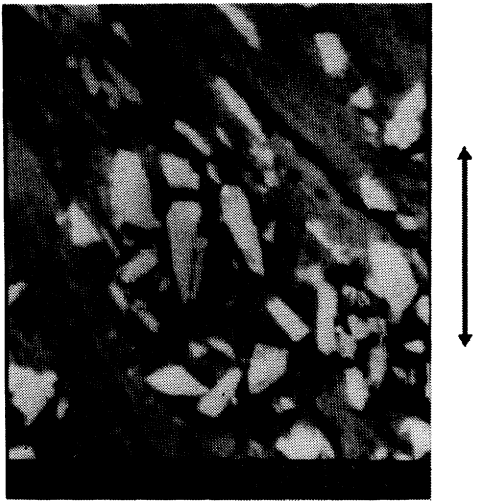

***Figure 4.*** *The SEM micrograph of microdamage occurred in 2124 Al/SiC$_p$ (3 μm SiC particles), where the arrow direction is loading direction.*

could be found in the deformed region and the fracture of the materials results from the accumulation of microdamage and localized deformation.

## 4. ANALYSIS AND DISCUSSION

### 4.1 About Flow Stress

The present experimental results showed that, under the same loading conditions, maximum flow stresses of current composites are different. The question is, what factors affect their flow stresses? Let's examine flow stress in composites according to some experimental results. In the present composites, their matrix is the same, 2124Al alloy, and the reinforcement is SiC particles with different sizes. During the whole deformation process, the flow stress level could be written as:

$$\sigma_f = f(E_m, \sigma_{mf}, d_m; E_p, d_p, \lambda_p, \rho) \tag{1}$$

in which, $E_m$, $d_m$, $\sigma_{mf}$ and $\rho$ are matrix Young's modulus, grain size, flow stress of matrix and the density of dislocation in matrix, respectively; $E_p$, $d_p$, $\lambda_p$ are particles' modulus, particle size, and edge-edge mean particle spacing between the two nearest neighboring particles, where $\lambda_p$ could be given by the following [17]:

$$\lambda_p = \frac{1}{2} d_p \left( \sqrt{\frac{2\pi}{3 f_v}} - \sqrt{\frac{8}{3}} \right)$$

in which, $f_v$ is volume fraction of SiC particles. According to the dimensional analysis [18], choosing $E_p$, $\sigma_{mf}$ and $\lambda_p$ as independent variations, the flow stress of composite can be written as:

$$\frac{\sigma_f}{\sigma_{mf}} = f\left(\frac{E_m}{E_p}, \frac{d_p}{\lambda_p}, \frac{d_m}{\lambda_p}, \frac{1}{\rho\lambda_p}\right) \tag{2}$$

Among the above, grain size, particle size and distance between the two nearest neighboring particles all have the length dimension, $L$, and $\rho$, $1/L$, i.e., $[d_m] = [d_p] = [\lambda_p] = L$ and $[\rho] = 1/L$. But in the present study, the matrix and reinforcement of the composites are given and the elastic modulus item is constant, $E_m/E_p$ = constant, thus

$$\frac{\sigma_f}{\sigma_{mf}} = f\left(\frac{d_p}{\lambda_p}, \frac{d_m}{\lambda_p}, \frac{1}{\rho\lambda_p}\right) \tag{3}$$

where $\lambda_p/d_p$ is the normalized distance between two nearest neighboring particles, $\rho\lambda_p$ is the total number of dislocations laid on the distance $\lambda_p$. Some microstructure scale parameters in the four materials are listed in the following:

| | $d_m$ (μm) | $\lambda_p$ (μm) | $\lambda_p/d_p$ | $\lambda_p/d_m$ |
|---|---|---|---|---|
| 2124Al alloy | 3–4 | — | — | — |
| 2124Al/SiC (3 μm) | 3–4 | 2.82 | 0.94 | 0.8 |
| 2124Al/SiC (13 μm) | 3–4 | 12.2 | 0.94 | 3.5 |
| 2124Al/SiC (37 μm) | 3–4 | 34.7 | 0.94 | 9.9 |

Noticing that, $\lambda_p/d_p$, the normalized distance between the two nearest neighboring particles is constant for the three composites and, for the same matrix, the grain size is given in these composites, Equation (3) could be written as:

$$\frac{\sigma_f}{\sigma_{mf}} = f\left(\frac{d_m}{\lambda_p}, \frac{1}{\rho\lambda_p}\right) \tag{4.a}$$

Therefore, the flow stress of the present composites is controlled by the spacing between the two nearest neighboring particles and the total number of dislocations laid on the distance as well as the size of matrix grains. Also, Equation (4) could be written as

$$\frac{\sigma_f}{\sigma_{mf}} = f\left(\frac{d_m}{\lambda_p}, \frac{d_m/d_m}{\rho\lambda_p}\right)$$

or

$$\frac{\sigma_f}{\sigma_{mf}} = f\left(\frac{d_m}{\lambda_p}, \frac{d_m/\lambda_p}{\rho d_m}\right) \tag{4.b}$$

In Equation (4.b), $\lambda_p/d_m$ is the grain number along distance $\lambda_p$ in matrix, $\rho d_m$ is the number of dislocations laid on one grain of matrix, or dislocations laid on the matrix. So the flow stress of these composites is controlled by the number of matrix grains between the two nearest neighboring SiC particles and the number of dislocations laid on one matrix grain. The larger $\lambda_p/d_m$ is, the lower the flow stress will be. If $\lambda_p/d_m \sim 1$, $\rho d_m$ is the only important factor governing the increase of flow stress. Now we could analyze the influence of dislocations to the flow stress in the composites. Let $\rho_{(3\ \mu m)}$ and $\rho_{(37\ \mu m)}$be the density of dislocation in the composites containing 3 or 37 micron SiC particles, respectively. Noticing, $\lambda_p \sim d_m$ and $\sigma_f \sim f(1/\rho_{(3\ \mu m)}\lambda_p)$ for the composite with 3 micron SiC particles; $\lambda_p \sim 10d_m$ and $\sigma_f \sim f(1/10, 1/\rho_{(37\ \mu m)}\lambda_p)$ for the composite with 37 micron SiC particles, we could obtain the following according to the experimental results $\sigma_{f(3\ \mu m)} > \sigma_{f(37\ \mu m)}$:

$$f\left(\frac{d_m}{\lambda_p}, \frac{1}{\rho_{(3\mu m)}\lambda_p}\right) > f\left(\frac{d_m}{\lambda_p}, \frac{1}{\rho_{(37\mu m)}\lambda_p}\right) \tag{5.a}$$

or

$$f\left(1, \frac{1}{\rho_{(3\mu m)} d_m}\right) > f\left(\frac{1}{10}, \frac{1/10}{\rho_{(37\mu m)} d_m}\right) \tag{5.b}$$

The results here showed that, if small SiC particles are large as the matrix grain which is comparable to the spacing between the two nearest neighboring particles, the flow stress increase in the composite is due to the influence of the dislocations laid on the spacing or dislocations in the matrix. But for the composite with large SiC particles, if the spacing between the two nearest neighboring particles is much larger than the matrix grain size, the particles' dispersing would be another main factor to influence the increased flow stress, which agreed with the previous research results [3,11,12]. Furthermore, formulas (3), (4) and (5) showed that normalized flow stress here is a function of an inverse power of ($\rho\lambda_p$) and $\lambda_p$, which is consistent with the conclusion in the previous research [13].

According to the experimental results, the whole deformation process could consist of two stages, elastic and plastic. Among them, $\sigma_{0.2}$ is important since it is not only the end of the elastic stage but also the beginning of the flow stage. Also, $\sigma_{0.2}$ is sensitive to the reinforced particles and it gets higher with decrease of particle size. On the other hand, for the present composites, their strain hardening de-

pends on that of matrix material only, so $\sigma_{0.2}$'s increasing would have a strong influence upon whole mechanical response of the present composites. The analysis above therefore could be applied to $\sigma_{0.2}$. Concerning strain hardening, we do not present more discussions in this paper and would like to describe deformation patterns occurring in these samples during plastic flow stage.

### 4.2 About Localized Deformation and Microdamage

Localized deformation, or an adiabatic shear band, is a description of the narrow region of highly local plastic deformation, which has been observed when materials are deformed at high strain rate, for example, in high speed metal forming or machining and so on. It results from several competing processes among which both strain-hardening and thermal softening are the main factors [19]. Extensive research has been directed to the understanding of shear localization, which is one of the main material instabilities, and significant progress has been made [20]. In recent years, Gray et al. [21] investigated the dynamic response of $MMC_p$ under high strain rate and Choi et al. [22] studied the forming conditions of adiabatic shear band occurring in $MMC_w$. Hirth et al. [13–15] applied a model to describe the localization evolution in $MMC_p$ and predicted an effective stress to cause shear band propagation. In the model, microstructure parameters, such as spacing of particles, dislocation and its Burgers length as well as the dislocation number, and shear band-particle interactions were accounted for. It was therefore shown to be consistent with several experimental observations. In this part, the focus is on the macromechanism of the localized deformation and deforming patterns caused by the effect of microstructure scales in the present composites.

Figure 2 and Figure 3 showed that, under the same loading ($\dot{\varepsilon} = 2100$ 1/s), the flow stress of the present materials has changed due to SiC particles and their deformation patterns in each material are different [Figures 3(a)–(d)]. One fact is that the composite with smallest SiC particles is of the highest flow stress and the localized deformation that occurred in the composite is much clearer than that which occurred in those with larger particles. The reason may be understood simply. As we know, in the composite containing small particles, the flow stress is highest and then its plastic work is greater than others. The localized deformation therefore occurs readily in this composite because the plastic work is prone to make localized deformation narrow [19]. In composites containing larger particles, these particles are too large to move. Furthermore, the development of strain localization may be more difficult in the composite containing larger SiC particles because the particles would block plastic flowing in the matrix. The observation agrees with the description in Hirth's research [15].

On the other hand, the size of SiC particles and the spatial distribution of these particles lead to different plastic flow patterns in the matrix, which has a very strong influence on the composites' constitutive response. Figure 3(d) shows that

such effect of SiC particle size on the plastic response is caused by the differences in constrained palstic flow of the ductile matrix. In particular, larger SiC particles with sharp corners lead to different plastic flow patterns within the matrix, or the plastic flows are interrupted and their orientations are changed randomly by the presence of hard particles. Obviously, as forenamed in this paper, different particle size distribution and spatial distributions would lead to different dislocation distributions in the matrix, the constraint on plastic deformation due to the interruption of plastic flow in the matrix would develop differently for different spatial distributions of the particles [see Figures 3(b) and (d)]. Furthermore, as analyzed in Reference [12], the plastic flow is increasingly interrupted and, consequently, the constraint on the matrix becomes more elevated and the stress-carrying in the plastic regime increases. In other words, dispersed smaller SiC particles could make the stress distribution more uniform and get its stress-carrying in each small plastic regime between particles, but with competing between strain-hardening and thermal softening, small SiC particles could not resist plastic flowing in the matrix more effectively than those larger SiC particles and localization is formed readily. Thus, in the composite with smaller SiC particles, deformation tends to concentrate along the maximum plastic flow and forms the localization band along where the macro-crack develops [Figure 3(b)].

Microdamage could be regarded as the result of two mechanisms, plastic deformation and thermal effect. It is well known that under high strain rate, the plastic deformation is no more an isothermal process so the temperature in the sample may rise very high. Additionally, at the localized deformation region, the temperature is higher than that in the other region. Therefore, the material at the narrow deformation region will encounter not only strong plastic flow but also higher temperature rising. According to the mechanical calculation analysis [2] and experimental observation, high stress concentration is always nearby sharp corners or interface. Thereby, in the composite with small particles, a lot of debonding could be found at sharp corners or the interface between particle and matrix in the localized deforming region (Figure 4).

## 5. CONCLUSIONS

The investigation on the 2124Al-alloy containing three different sizes of SiC particles and 2124Al alloy under dynamic compression was presented in this paper. Experimental and analytic results show that the microstructure effect, such as matrix grain size, particle size, edge-edge particle spacing between two neighboring particles and the dislocation concentration along the spacing have a pronounced effect on the overall mechanical response of the present composites. Some conclusions are listed below:

1. Under current loading ($\dot{\varepsilon} = 2100$ 1/s), for SiC particles with different sizes, the

flow stress of present materials increases in the following order: 2124 Al alloy → 2124Al/$SiC_p$ (37 μm) → 2124Al/$SiC_p$ (13 μm) → 2124Al/$SiC_p$ (3 μm). Although, during the whole deformation process, most of the stress increase in the present composites is due to the strain hardening which depends on that of the matrix material. SiC particles have a strong effect on the $\sigma_{0.2}$ of composites and they increase in the order: 2124Al alloy → 2124Al/$SiC_p$ (37 μm) → 2124Al/$SiC_p$ (13 μm) → 2124Al/$SiC_p$ (3 μm).

2. The normalized flow stress in current composites has been presented by the dimensional analysis. It is a function of an inverse power of edge-edge particle spacing, dislocation density and matrix grain size, which supports the previous research results [13–15].
3. For the composite with small SiC particles, the flow stress level is controlled only by dislocations laid on the matrix, while SiC particles size, matrix grain size and spacing between two neighboring particles are comparable to each other, and for composites with large SiC particles, if spacing between the two neighboring particles is much greater than the matrix strain size, the particles' dispersing would be another main factor to influence the increased flow stress.
4. Localized deformation more readily formed in the composite with small SiC particles under the same loading, which is due to the plastic work stored in materials. On the other hand, it related to the effect of SiC particle size on the plastic response which is caused by the differences in constrained plastic flow of the ductile matrix. That is to say, larger SiC particles could resist more effectively the plastic flow in the matrix than small particles so that the composite reinforced with larger SiC particles can be subjected to higher loading.
5. The voids in the matrix nearby sharp corners or interface debonding between particle and matrix always occurred in the deformed region, which would result from the strong plastic deformation and higher temperature difference.

## ACKNOWLEDGMENTS

This research is supported by NSFC under Grant No. 19672068 and Major Project of CAS-"KJ951-1-201." The author acknowledges the advice of Professor YL Bai and Professor SD Zhao, and would also like to thank LM Luo and H Shen for their assistance in experimental work.

## REFERENCES

1. Clyne, T.W. and Withers, P.J. 1992. *An Introduction to Metal Matrix Composites,* Cambridge University Press, Cambridge.
2. Christman, T., Needleman, A. and Suresh, S. 1989. "An Experimental and Numerical Study of Deformation in Metal-Ceramic Composites," *Acta. Metall.* 37:3029–3050.
3. Edelson, B.I. and Baldwin, W.M., Jr. 1962. "The Effects of Second Phases on the Mechanical Properties of Alloys," *Transaction of ASM,* 55:230–250.

4. Cheng, C.M. 1982. "Fracture and Mechanics of Continua Media," *Advances of Mechanics,* 12:133–140 (in Chinese).
5. Hong, Y.S., Ye, Y.G. and Xia, X.X. 1983. "The Effects of the Size of the Second Phase Particles on the Mechanical Properties of a Low Alloy Steel," *Mechanical Behavior of Materials, Proceedings of ICM 4,* Eds. J. Carlsson and N.G. Ohlson, 2:849–855.
6. Eshelby, J.D. 1957. "The Determination of the Elastic Field on an Ellipsoidal Inclusion and Related Problems," *Proc. R. Soc. Lond.* A241:376–396.
7. Mura, T. 1987. *Micromechanics of Defects in Solids,* (2nd ed.) Martinus Nijhoff, Dordrecht.
8. Llorca, J., Needleman, A. and Suresh, S. 1991. "An Analysis of the Effects of Matrix Void Growth on Deformation and Ductility in Metal-Ceramic Composites," *Acta. Metall. Mater.* 37:2317–2335.
9. Tvergaard, V. 1990. "Analysis of Tensile Properties for Whisker-Reinforced Metal Matrix Composites," *Acta. Metall. Mater.* 38:185–194.
10. Needleman, A. and Tvergaard, V. 1993. "Comparison of Crystal Plasticity and Isotropic Hardening Prediction for Metal-Matrix Composites," J. Applied Mech. 60:70–76.
11. Shen, Y.-L., Finot, M., Needleman, A. and Suresh, S. 1994. "Effective Elastic Response of Two-Phase Composites," *Acta. Metall. Mater.* 42:77–97.
12. Shen, Y.-L., Finot, M., Needleman, A. and Suresh, S. 1995. "Effective Plastic Response of Two-Phase Composites," *Acta. Metall. Mater.* 43:1701–1722.
13. Kamat, S.V., Hirth, J.P. and Mehrabian, R. 1989. "Mechanical Properties of Particulate-Reinforced Aluminum-Matrix Composites," *Acta. Metall. Mater.* 37:2395–2402.
14. Kamat, S.V., Rollett, A.D. and Hirth, J.P. 1991. "Plastic Deformation in Al-Alloy Matrix-Alumina Particulate Composites," *Scripta Metall. Mater.* 25:27–32.
15. Hirth, J.P. 1992. "A Model for a Propagating Shear Band on the Basis of a Tilt Wall Dislocation Array," *Applied Mech. Rev.* 45:s71–s74.
16. Hauser, F.E. 1966. "Techniques for Measuring Stress-Strain Relations at High Strain Rates," *Exp. Mech.* 6:395–402.
17. Roy, G.L.E., Embury, J.D., Edward, G. and Ashby, M.F. 1981. "A Model of Ductile Fracture Based on the Nucleation and Growth of Voids," *Acta. Metall.* 29:1509–1522.
18. Sedev, L.I. 1959. *Dimensional and Similarity Methods in Mechanics* (translated), Infosearch, London.
19. Bai, Y.L. and Dodd, B. 1992. *Adiabatic Shear Localization,* Pergamon Press, Oxford.
20. Needleman, A. and Tvergaard, V. 1992. "Analysis of Plastic Flow Localization in Metals," *Applied Mech. Rev.* 45:s3–s18.
21. Hong, S.I., Gray III, G.T. and Lewandowski, J.J. 1993. "Dynamic Deformation Behavior of Al-Zn-Mg-Cu Alloy Matrix Composites Reinforced with 20% SiC," *Acta. Metall. Mater.* 41:2337–2351.
22. Lee, S., Cho, K.-M., Kim, K.C. and Choi, W.B. 1993. "Adiabatic Shear Band Formation in Al-SiC$_w$ Composites," *Metall. Trans.* 24A:895–900.